PUBLICATION P3

RF MEMS Impedance Tuners for 6–24 GHz Applications

Accepted for publication to International Journal
of RF and Microwave Computer-Aided
Engineering, February 2006.

Accepted for publication in International Journal of RF and Microwave Computer-Aided Engineering, Feb. 2006

RF MEMS Impedance Tuners for 6-24 GHz Applications

Tauno Vähä-Heikkilä[1,2], Koen Van Caekenberghe[2], Jussi Varis[1], Jussi Tuovinen[1] and Gabriel M. Rebeiz[2,3]

[1]MilliLab, VTT Technical Research Centre of Finland, P.O. BOX 1000, 02044 VTT, Finland, tauno.vaha-heikkila@vtt.fi

[2]The University of Michigan, Electrical Engineering and Computer Science Department, Ann Arbor, MI, 48109-2122, USA

[3]University of California at San Diego, Electrical and Computer Engineering Department, La Jolla, 92037, CA USA, rebeiz@ece.ucsd.edu

ABSTRACT

RF MEMS tuners with wide impedance coverage have been developed for 6-24 GHz noise parameter and load-pull measurement systems. The tuners are based on triple-, double-, and single-stub topologies loaded with switched MEMS capacitors. Several designs are presented, and they use 10-13 switched MEMS capacitors to produce 1024 to 8192 (2^{10}-2^{13}) different impedances. The measured impedance coverage agrees well with simulations and it is the widest ever measured impedance coverage from any planar tuner to-date.

Keywords: RF MEMS, impedance tuner, noise parameters, load-pull, matching network, antenna tuner

I. INTRODUCTION

Impedance tuners are commonly used in both load-pull and noise parameter measurements of transistors at microwave and mm-wave frequencies, e.g. [1-3]. Typically, these are mechanical devices with either coaxial or waveguide structures, and use motors for automatic control. Tuners are also made using diodes and transistors, but these designs are lossy and result in a limited impedance coverage [4,5]. Also, they add electronic noise which makes accurate noise measurements more challenging. RF MEMS impedance tuners with low loss and large impedance coverage are therefore desirable to increase measurement automation and accuracy. Also, MEMS-based impedance tuners are small enough to be mounted inside an on-wafer probe. An impedance tuner can either be of the transmission or reflection-type (Fig. 1) design, and typical impedance tuners are based either on double-stub [6,7] or triple-stub topologies [8,9]. The stub topologies are not ideal for power amplifier applications since they result in a higher loss compared to loaded-line tuners introduced by Vähä-Heikkilä and Rebeiz in [10,11]. Also, Shen and Barker have presented a distributed type double slug impedance tuner with low loss [12]. Still, the stub-based tuners result in excellent impedance coverage over a wide frequency range as well as high voltage standing wave ratios (VSWR), and are suitable to be used as noise parameter or load-pull impedance tuners.

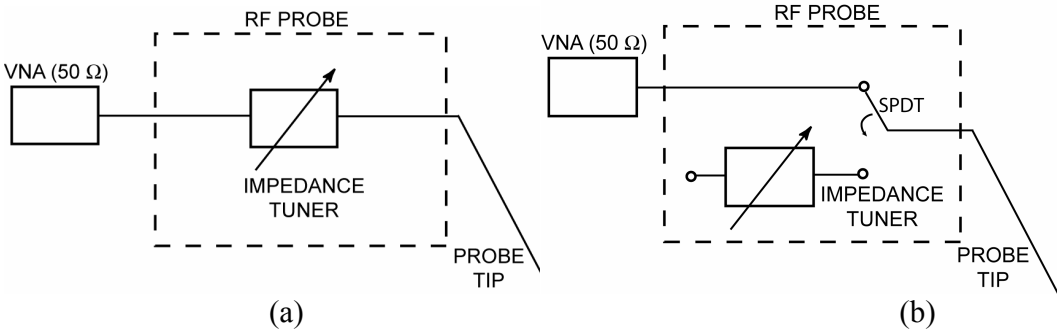

Figure 1. a) Transmission and b) reflection-type impedance tuner inside an RF probe used in on-wafer measurements.

In this work, impedance tuners based on switched MEMS capacitors are presented. The goal is not only to achieve a wide impedance coverage, but also to achieve this over a wide frequency range. This is done using a novel idea based on changing the electrical length *and* separation between the tuning stubs with the switched capacitor approach. The impedance and electrical length of the stub is also changed using MEMS switched capacitors. This method results in 2^N different impedances over a wide frequency range for a stub circuit loaded with N different switched capacitors.

II. TUNER DESIGN

An RF MEMS switch in series with a fixed metal-air-metal (MAM) capacitor is the basic building block of the stub-based tuners. There are several parameters which affect the impedance coverage of impedance tuners: the number and capacitance values of the switched MEMS capacitors have the most important effect on the tuning range and bandwidth. Other selectable parameters are the spacing of the switched capacitors, the transmission-line (t-line) properties (Z_0, ε_{reff}), the distance between the stubs, and the lengths of the stubs.

The single-, double-, and triple-stub designs are optimized using Agilent ADS[1] to obtain as large a tuning range and bandwidth as possible with the minimum number of switched MEMS capacitors. We have not found a closed-form design technique since there are many design parameters for impedance tuners. Some design insights are given later in the paper. The equivalent circuit of the switched MEMS capacitor is shown in Fig. 2, and the component values are presented in Table 1. The up-state capacitance of the switched capacitor is determined mostly by the up-state capacitance of the MEMS switch, and the down-state capacitance is determined by the two MAM capacitors [11].

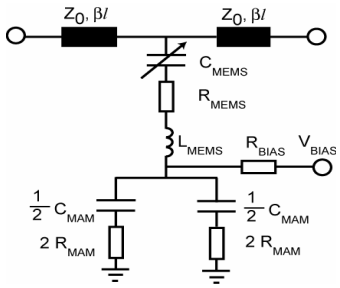

Figure 2. Equivalent circuit of a switched MEMS capacitor (unit cell in tuner design).

Fig. 3 shows a fabricated switched MEMS capacitor on a coplanar waveguide (CPW) t-line on a glass substrate (Corning 7040). The fabrication process is based on standard surface MEMS techniques and is described in [13]. The dimensions of the gold MEMS switch are 280 μm x 80 μm x 0.8 μm, and it is suspended 1.1 μm above the t-line. A 3500 Å silicon nitride layer was used as a dielectric interlayer. The circuit is electroplated to 3 μm thickness (except the MEMS bridges) to reduce the t-line and MAM capacitor loss. SiCr bias lines with resistance of 700 Ω/square are used for actuating the MEMS switches. The measured pull-down voltage is 15-17 V, and a bipolar actuation voltage of +/-35 V was used for obtaining an excellent metal-to-dielectric contact in the down-state position.

[1] Advanced Design System 2002, Agilent Technologies, Santa Clara, CA, USA, 2002.

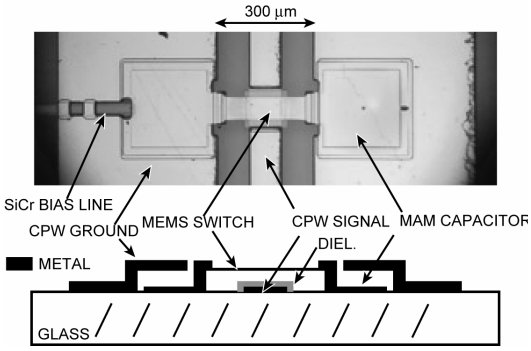

Figure 3. Picture and cross-sectional view of a switched MEMS capacitor unit cell.

TABLE 1. Measured t-line properties from the trl calibration and fitted values for the switched MEMS capacitor.

ε_r	4.6
Z_0 (Ω) (100/100/100 μm)	86.2
ε_{reff}	2.72
α (dB/cm), 10/20 GHz	0.35/0.52
C_{MEMS} Up-State (fF)	91
C_{MEMS} Down-State (fF)	750
R_{BIAS} (kΩ)	> 3
L_{MEMS} (pH)	9.5
R_{MEMS}+ R_{MAM} (Ω)	0.6
C_{MAM} (fF)	850

As seen in Table 1, the measured capacitance ratio of the RF MEMS switch is only 8:1 due to its low height and the thick silicon-nitride layer. The total up-state and down-state capacitances of the switched capacitor are C_U = 82.2 fF and C_D = 398 fF, respectively, resulting in a capacitance ratio of 4.9:1. The quality factor of the switched MEMS capacitor is calculated using $Q = (2\pi fC(R_{MEMS}+ R_{MAM}))^{-1}$ and at 12 GHz, results in an up and down-state values of Q_U = 269 (C_U = 82.2 fF, X = -j161 Ω) and Q_D = 55 (C_D = 398 fF, X = -j33.3 Ω), respectively. Table 2 summarizes the properties of the entire unit cell of Fig. 3. The unit cell has 31 degree phase change between its up and down-states at 12 GHz.

TABLE 2. Properties of the unit cell.

Length (μm)	480
Z_0 (Ω)	86.2
Z_U (Ω)	45
Z_D (Ω)	23
ϕ_U(degree) at 12 GHz	-22.3
ϕ_D(degree) at 12 GHz	-53.2
Q_U at 12 GHz	269
Q_D at 12 GHz	55

The reconfigurable triple-, double-, and single-stub impedance tuners were optimized to have 10-13 identical switched MEMS capacitors (S1-S13). The number of switched capacitors (N) has great effect to the impedance coverage of the tuners. By using a larger number of switched capacitors better impedance coverage can be achieved at the cost of a more complicated control system and higher circuit loss.

The switched capacitors were used for tuning the electrical lengths of the stubs and also the separation between them. Spacing between the stubs is 3.0 mm for the double- and triple-stub designs (Figs. 4-7). It should be noted that a small capacitance ratio does not result in a large tuning range at the lower frequencies, but on the other hand, a high capacitance ratio causes a short circuit at higher frequencies. Therefore, the circuits were optimized with a large number of simulations in ADS, and the best capacitance ratio was found to be between 4 and 10.

There is truly a large number of circuit combinations which can offer a wide frequency coverage and wide tuning range, and in this paper, we will present four representative circuits based on triple (Figs. 4 and 5), double (Fig. 6), and single-stub (Fig. 7) designs. Notice that the double-stub design is physically rather small, and owes its wide tuning range to the use of 3 switched capacitors between the stubs.

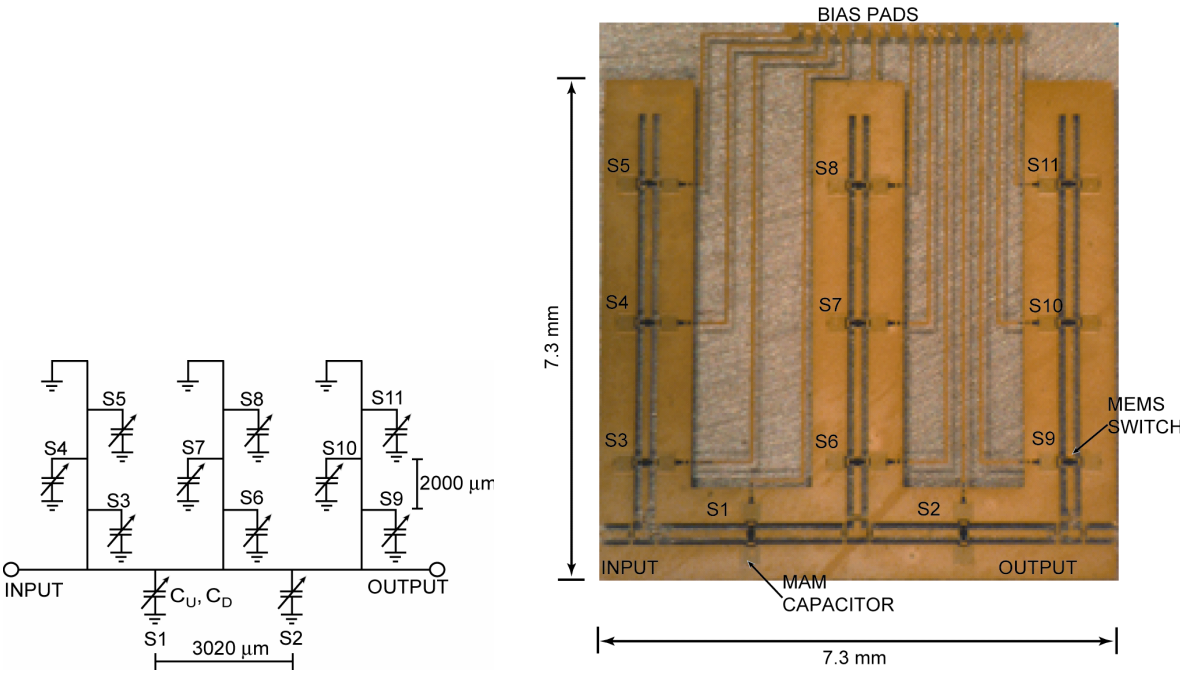

Figure 4. a) Circuit diagram and b) picture of the 6-20 GHz reconfigurable triple-stub RF MEMS impedance tuner with 11 switched MEMS capacitors (S1-S11). Notice that the stubs are short circuited.

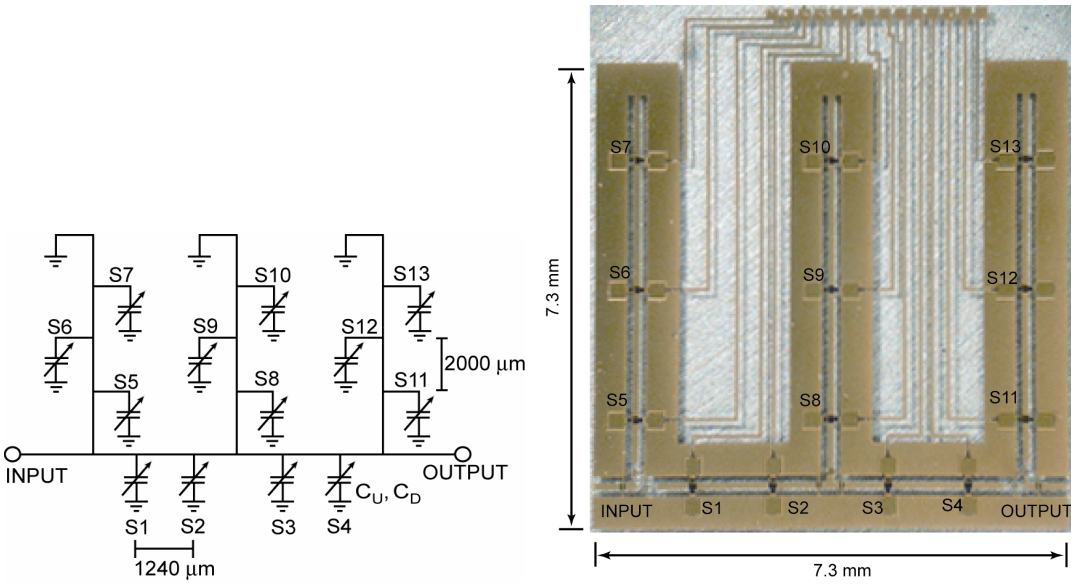

Figure 5. a) Circuit diagram and b) picture of the 6-20 GHz reconfigurable triple-stub RF MEMS impedance tuner with 13 switched MEMS capacitors (S1-S13). Note that 2 switched capacitors are used between the stubs and the stubs are short circuited.

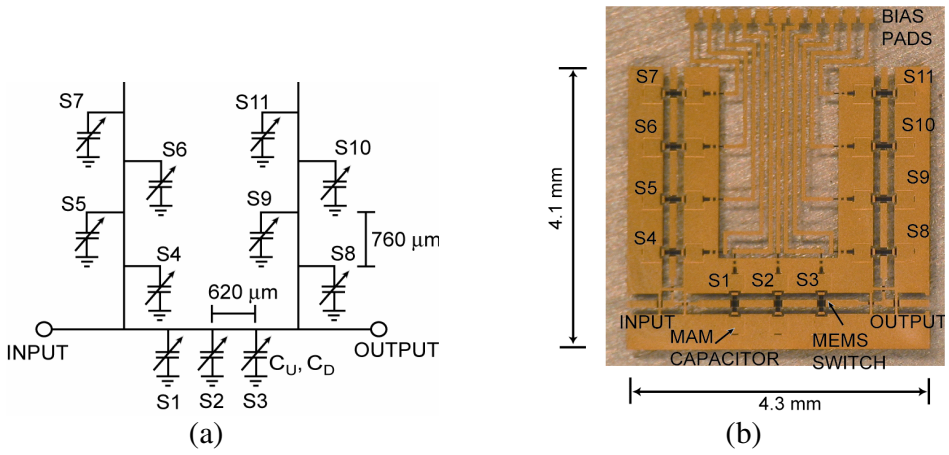

Figure 6. a) Circuit diagram and b) picture of the 4-30 GHz double-stub RF MEMS impedance tuner with 11 switched MEMS capacitors (S1-S11). Notice that three switched capacitors are used between the stubs, and that the stubs are open circuited.

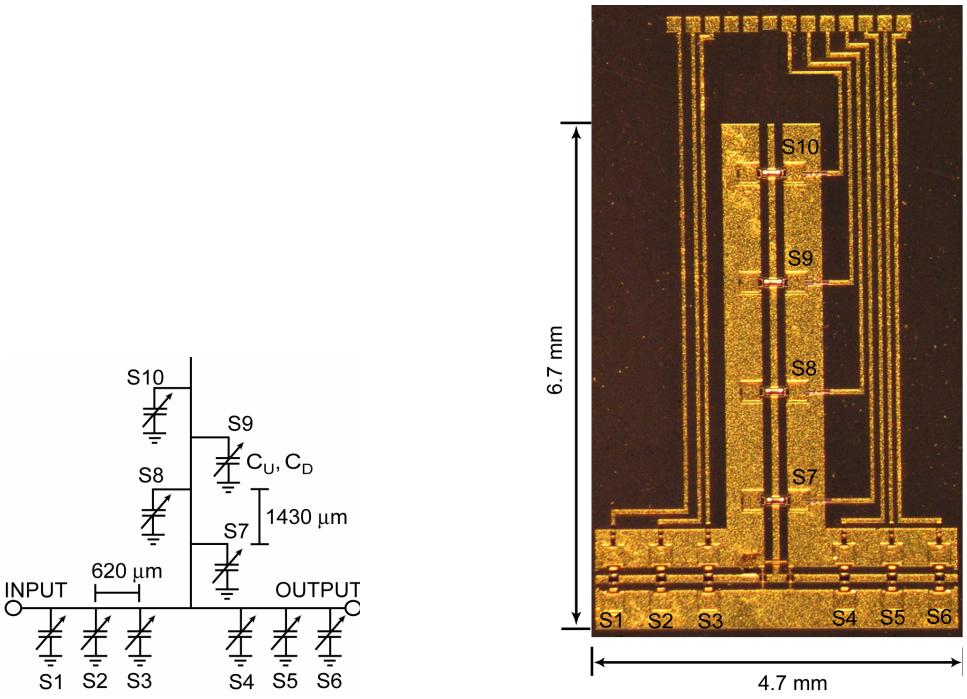

Figure 7. a) Circuit diagram and b) picture of the 6-25 GHz single-stub RF MEMS impedance tuner with 10 switched MEMS capacitors (S1-S10). Notice that three switched capacitors are placed both before and after the stub.

III. CIRCUIT MODEL

An accurate circuit model of the tuner is very important in predicting the impedance coverage and behavior over a wide frequency range. Also, the tuners have 10 to 13 switched capacitors producing 1024-8192 different impedances making it time consuming to measure all the different combinations. The circuit models were developed by first measuring several switched MEMS capacitors both as single elements and as elements in a distributed (loaded-line) network as in [11], and deriving the equivalent circuit of the unit-cell switched capacitor (see Fig. 2 and Tables 1-2). To get accurate models for the T-junctions, they were simulated with the Sonnet2 full wave EM simulator as three port elements, and also having air bridges crossing each arm. The unit cell, the Sonnet models of the T junctions, and the t-line characteristics were all used in Agilent ADS for predicting the response of the whole network under different switch combinations. The accuracy of the model is clearly seen with a comparison between the simulated and measured S-parameters for the triple- and double-stub tuners in Figs. 8 and 9. The models agree for all switch combinations which were tested, but only two representative conditions are shown in Figs. 8 and 9.

[2] Sonnet, ver. 8.52, Sonner Software Inc., Syracuse, NY, 1986-2001.

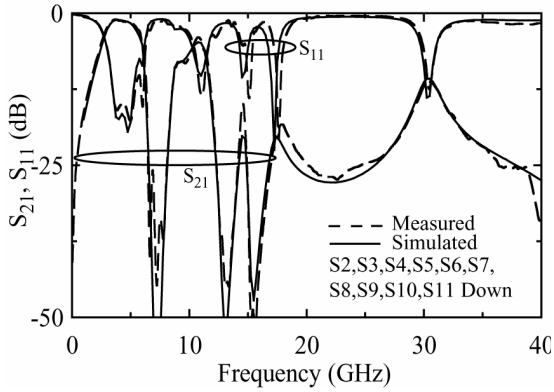

Figure 8. Measured and simulated S-parameters for the triple-stub tuner of Fig. 4 with 11 switches, when switches S2, S3, S4, S5, S6, S7, S8, S9, S10, and S11 are in the down-state.

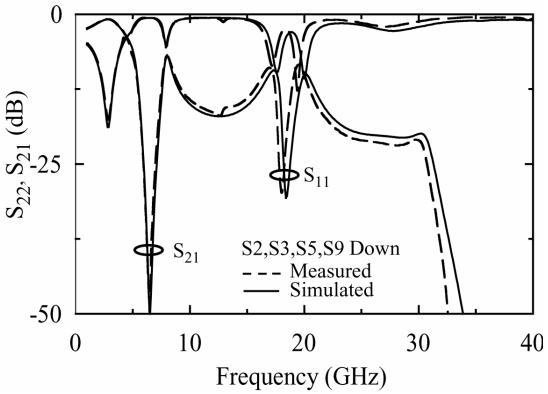

Figure 9. Measured and simulated S-parameters for the double-stub tuner of Fig. 6 with 11 switches, when switches S2, S3, S5, and S9 are in the down-state.

IV. IMPEDANCE COVERAGE

A. Triple-Stub Tuner with 11 Switched Capacitors

The measured (160) and simulated (2^{11} =2048) impedance points of the reconfigurable triple-stub tuner are presented in Fig. 10 at 6-20 GHz. In this case, a 50 Ω load was placed at the output port, and the input reflection coefficients were measured with different switches actuated into the down-state position. Due to the number of points in the measurement set-up, it is hard to show a 1:1 mapping between the measured and simulated data, but they agree quite well with each other (see also Figs. 8 and 9). It can be seen that the obtained impedance coverage is good for noise-parameter or load-pull measurements. There is some discrepancy at 20 GHz, and this is when the triple-stub network is quite large and the CPW lines are starting to radiate, which is not modeled by Agilent ADS.

The network can also be used for matching a low-impedance load (10 Ω) at virtually all frequencies between 6 and 20 GHz, but as will be seen in Section V, the triple stub tuner results in higher loss compared to other designs [9].

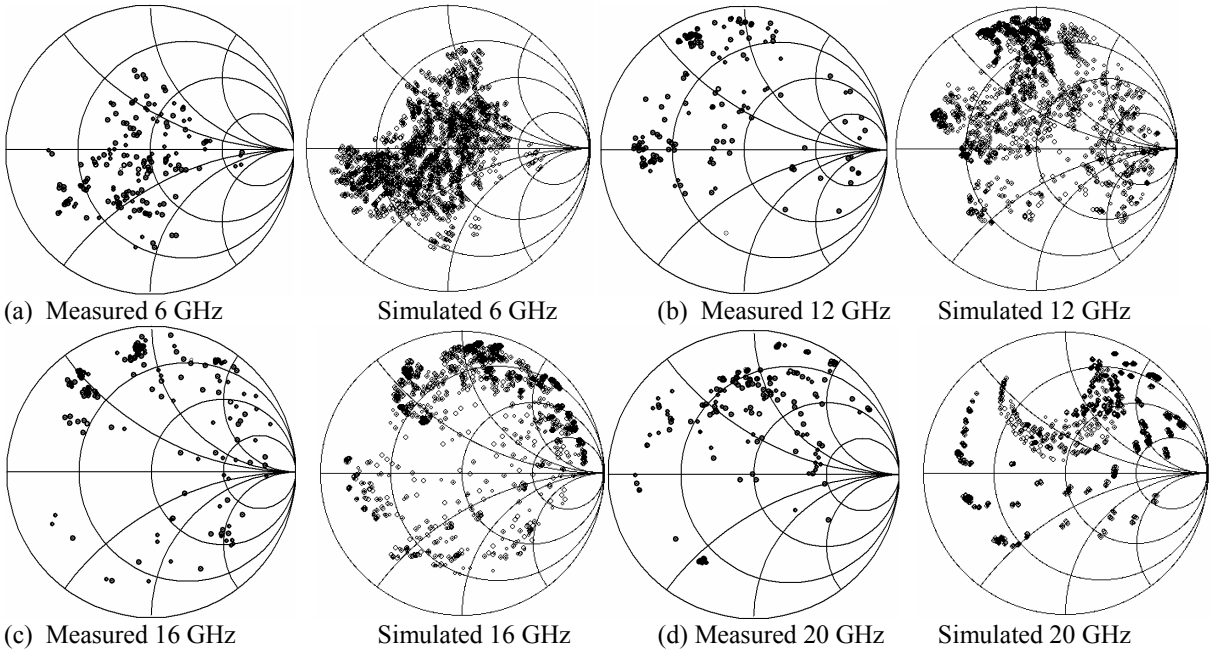

Figure 10. (a)-(d) Measured (160 points) and simulated (2048 points) impedance coverage of the triple-stub tuner with 11 switched capacitors.

The triple-stub tuner with 11 switches can also be used in a reflection-mode with open or short-circuit termination at the output port (see Fig. 1) for obtaining wide impedance coverage (Fig. 11). This is useful in noise parameter measurements, and in this case, an important characteristic is to get a near-circular impedance locus on the Smith chart [14].

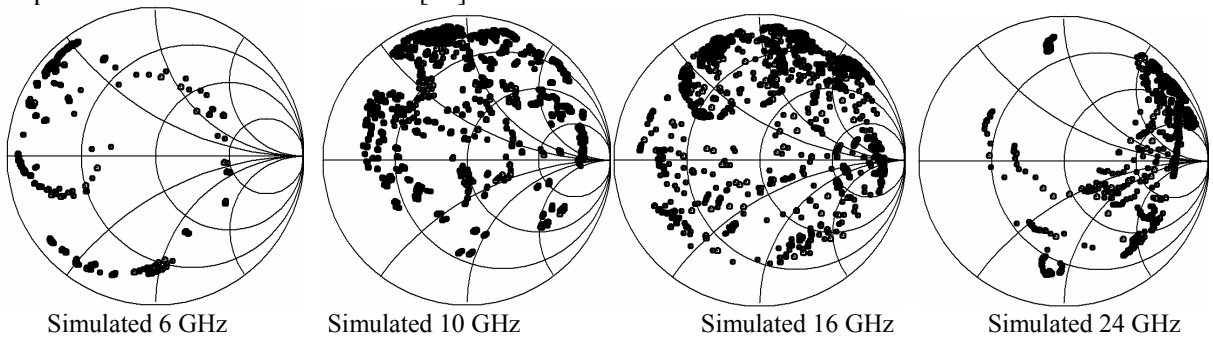

Figure 11. Simulated (2048 points) impedance coverage of the triple-stub tuner when the output terminated with an open circuit. Similar results are achieved for a short-circuit termination.

B. Triple-Stub Tuner with 13 Switched Capacitors

The triple-stub tuner was also optimized for 13 switched capacitors. Two additional switched capacitors were placed between the stubs to result in a higher tuning (2 bit instead of 1-bit) range for the electrical distance between the stubs. This tuner results in 8192 (2^{13}) different impedances, and its measured (160 points) and simulated impedance coverage with a 50 Ω load at the output port are shown in Fig. 12. Also, the simulated impedance coverage with the output terminated with an open circuit is shown in Fig. 13. It

is seen that the impedance coverage with the 50 Ω load is not much wider compared to the design with 11 switched capacitors, but better impedance coverage can be achieved with the output terminated either with an open or a short circuit (reflection mode).

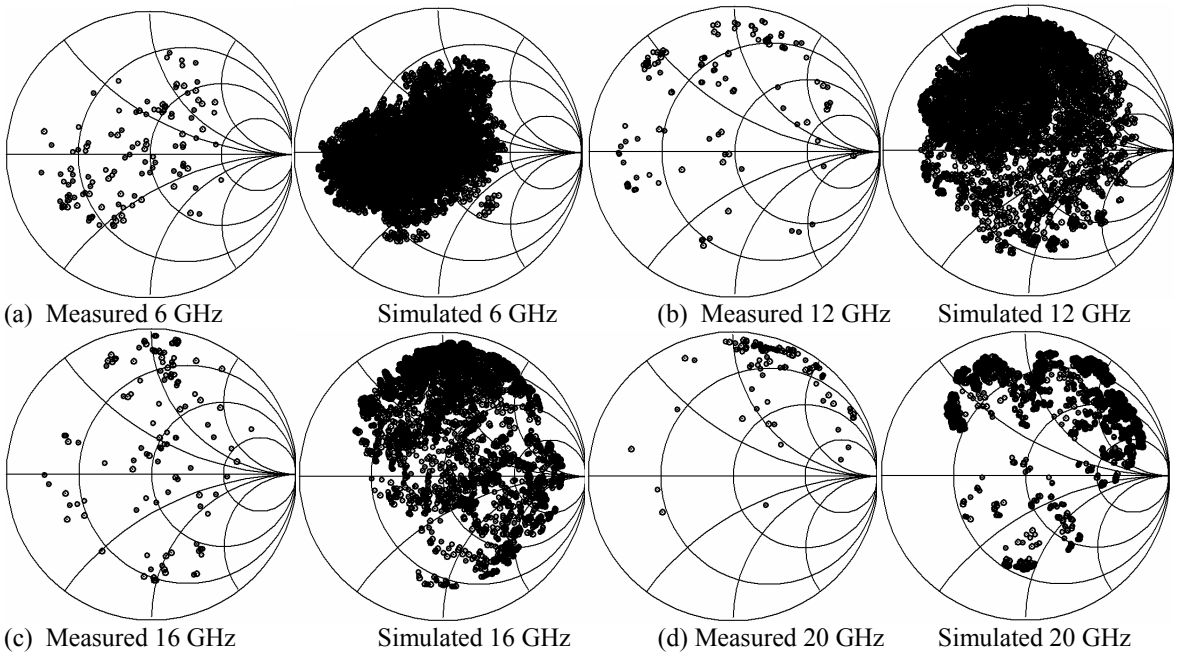

Figure 12. (a)-(d) Measured (160 points) and simulated (8192 points) impedance coverage of the triple-stub tuner with 13 switched capacitors with a 50 Ω load.

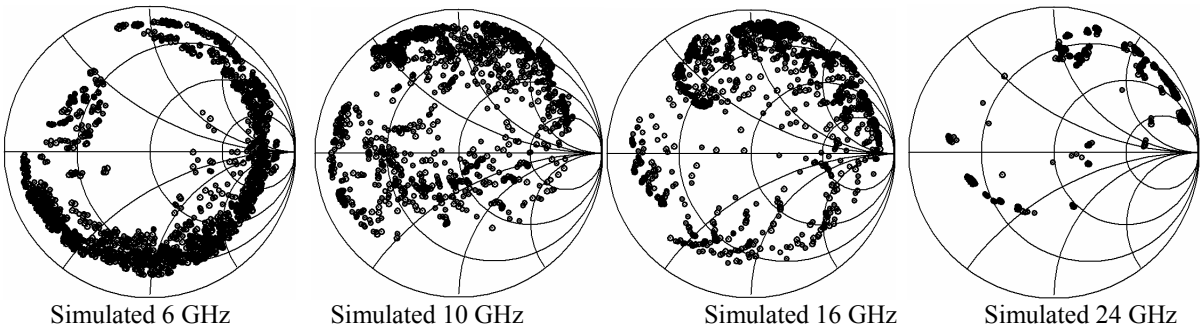

Figure 13. Simulated (8192 points) impedance coverage of the triple-stub tuner with 13 switched capacitors when the output is terminated with an open circuit (reflection mode). Similar results are achieved for a short-circuit termination.

C. Double-Stub Tuner with 11 Switched Capacitors

The measured (160) and simulated (2048) impedance points for the double-stub tuner are shown in Fig. 14 at 4-30 GHz. The impedance coverage of the double-stub tuner is not as wide as the impedance coverage of the triple-stub tuners at 6-20 GHz, but on the other hand, it is much better above 20 GHz. Notice that the impedance coverage at 6 GHz is very small and this is due to the value of the switched capacitors and a resonant phenomena which is occurring at 6 GHz due to the size of the double-stub tuner (this is not

observed at 4 or at 8 GHz). Our simulations clearly indicate that this can be mitigated by changing the values of the switched capacitor to be C_U = 50 fF and C_D = 750 fF, but at the expense of a reduction in the tuning range to 18 GHz.

Fig. 15 shows that even with the double-stub topology and an open-circuit termination at the output (reflection mode), it is possible to achieve as good impedance coverage as with the triple-stub tuners over a wide frequency range.

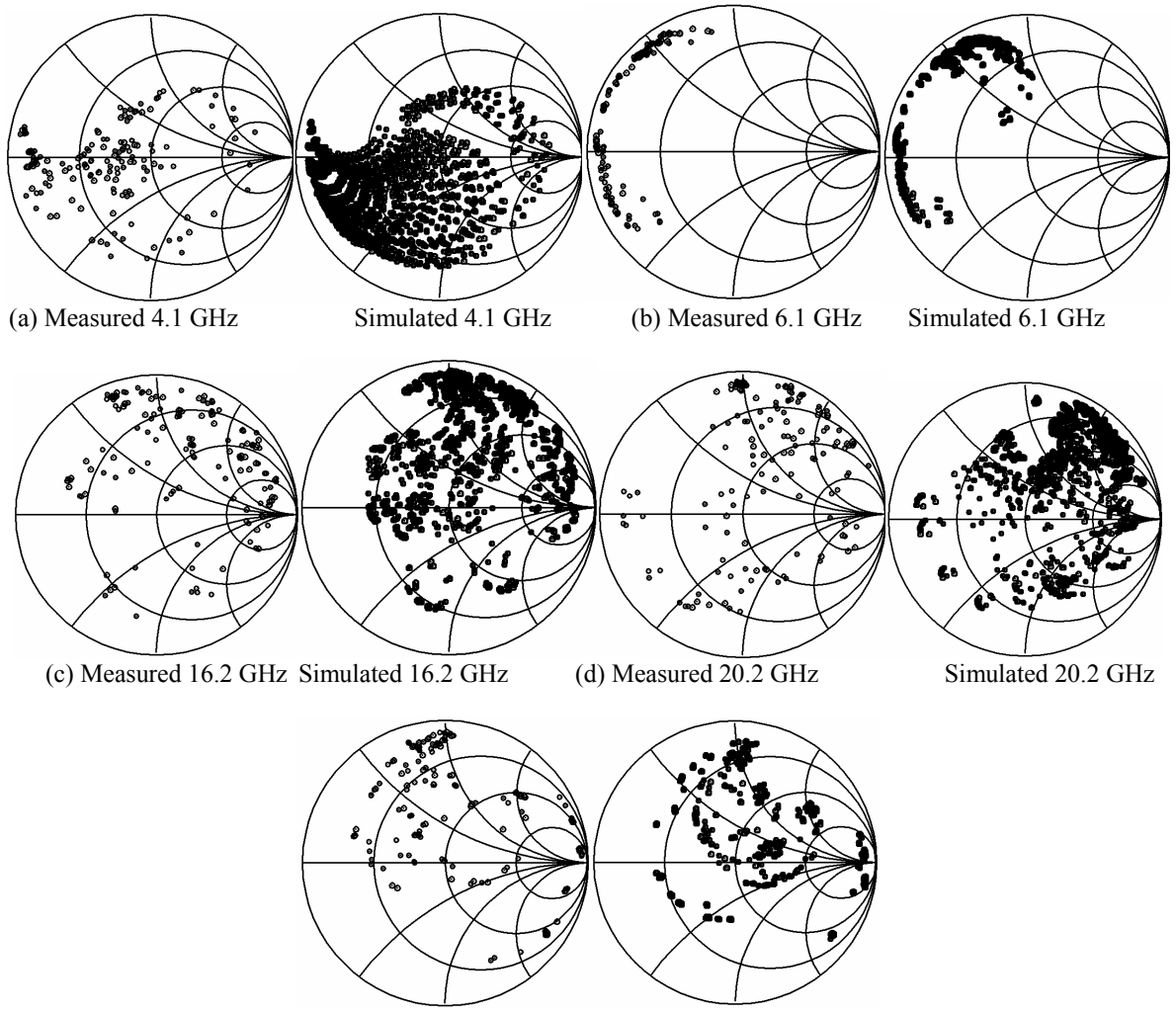

Figure 14. (a)-(f) Measured (160 points) and simulated (2048 points) impedance coverage of the double-stub tuner with 11 switched capacitors with a 50 Ω load.

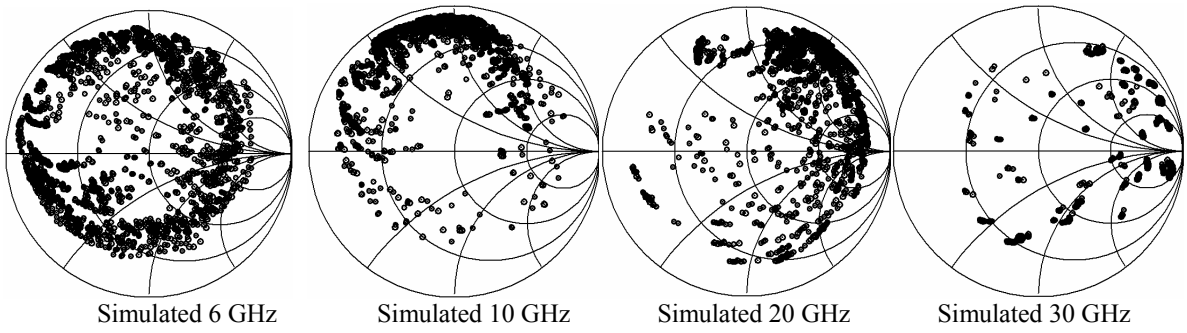

Figure 15. Simulated (2048 points) impedance coverage of the double-stub tuner when the output terminated with an open circuit (reflection mode). The impedance coverage is the same at 10-30 GHz for a short circuit termination and with a slightly reduced coverage at 6 GHz.

D. Single-Stub Tuner with 10 Switched Capacitors

Measured (90 points) and simulated (1024 points) impedance coverage of the single-stub tuner with an open circuited is presented in Fig. 16 at 6-20 GHz. The single-stub tuner does not have the frequency bandwidth of the triple-stub design showing only good impedance coverage between 10 and 20 GHz. Still, these are excellent results from a single-stub design, and is due to the variable impedance and electrical-length loading of the switched capacitors which are not only used in the stub, but also in the t-line before and after the stub. A single-stub tuner with a short circuited stub was also realized. It has as good impedance coverage as with the open circuited single-stub tuner. Our simulations indicate that the single-stub tuner with a 50 Ω load can be improved by using switched capacitors having a higher capacitance ratio with C_U = 50 fF and C_D = 800 f. It will be seen in Section V that the single stub tuner results in the lowest loss matching network out of all the cases presented above (for power amplifier applications).

Finally, if the network is terminated with an open or short circuit (reflection mode), one can obtain a very good impedance coverage at 6-24 GHz (Fig. 17).

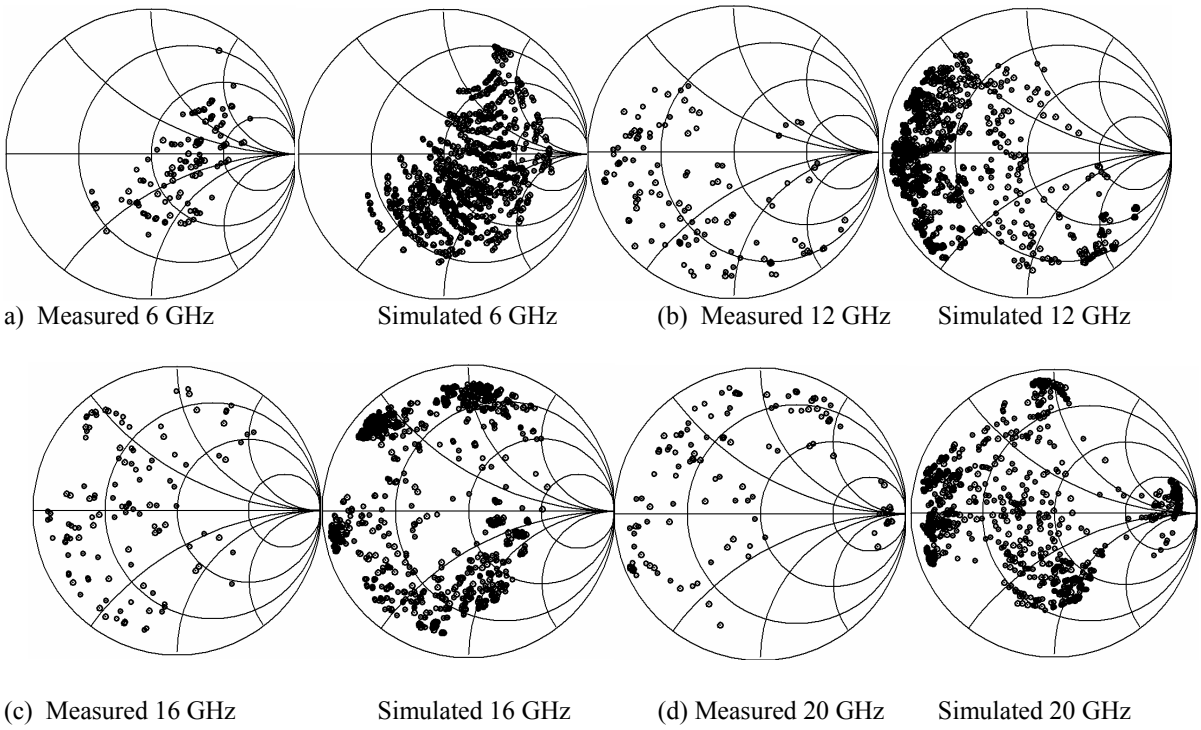

Figure 16. (a)-(d) Measured (90 points) and simulated (1024 points) impedance coverage of the single-stub tuner with a 50 Ω load.

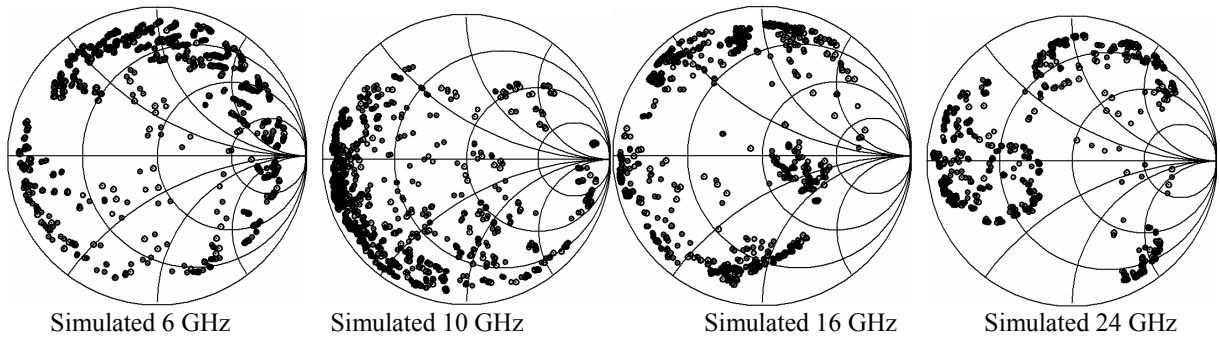

Figure 17. Simulated (1024 points) impedance coverage of the single-stub tuner when the output terminated with an open circuit (reflection mode). The impedance coverage is the same at 10-30 GHz for a short circuit termination but results in reduced coverage at 6 GHz.

V. CASE STUDY: MATCHING OF A 20 Ω LOAD TO 50 Ω

The circuit model developed above can be used for analyzing different matching conditions. A 20 Ω load was matched to 50 Ω with the triple, double, and single-stub tuners at 4-20 GHz and different switch combinations were chosen to achieve an impedance match better than -19 dB at different frequencies. Fig. 18 shows the case of the single-stub tuner, where the loss is defined as $1 - |S_{11}|^2 - |S_{21}|^2$ and includes the ohmic loss in the t-line and bridges, and radiation loss. The single-stub tuner is well suited for matching applications up to 16 GHz with a loss of 0.1-0.2 (90-80% efficient which is 0.5-1 dB of loss). However, the loss is quite high in the triple- and double stub tuners at 6-20 GHz (1-2 dB loss) and is not shown. The

reason is that these networks are quite large and include two or three T-junctions. Therefore, double and triple-stub tuners are better suited for noise parameter and load-pull measurement applications.

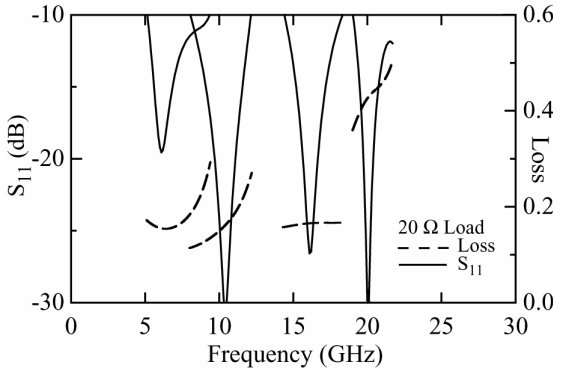

Figure 18. Simulated input reflection coefficient and loss of the single-stub tuner with 10 switched capacitors at 6, 10, 16, and 20 GHz with a 20 Ω load matched to 50 Ω. Simulations were done based on the circuit model (which agrees very well with measurements). Switches S3, S4, S5, S7, S9, and S10 were down when matching at 6 GHz, S5 and S10 at 10 GHz, S8 and S10 at 16 GHz, and S4, S5, and S8 at 20 GHz.

VI. MEASURED $|\Gamma_{MAX}|$

A figure of merit for impedance tuners is the maximum achievable reflection coefficient, $|\Gamma_{MAX}|$, and the measured $|\Gamma_{MAX}|$ values for the tuners are shown in Table 3 (for the 90-160 points out of 1024-8192 possible). These measurements show that the double-stub tuner design with three switched capacitors between the stubs results in a measured $|\Gamma_{MAX}| > 0.9$ for the whole frequency band, and the best measured $|\Gamma_{MAX}|$ is 0.99 at 30 GHz, which is equal to VSWR of 199. The measured $|\Gamma_{MAX}|$ values are comparable to previously published integrated impedance tuners. Some notable results were: A VSWR of 6 at 27 GHz [4], a VSWR of 12.3 at 27 GHz [5], a VSWR of 32.3 at 30 GHz [6], and a VSWR of 99 at 20 GHz [7]. However, all of the tuners in [4-7] were quite narrowband as opposed to the wideband designs presented here.

TABLE 3. Measured $|\Gamma_{MAX}|$ for the difference tuners for 90-160 points with 50 Ω terminations. Higher $|\Gamma_{MAX}|$ could be achieved if more measurements points were taken.

Frequency (GHz)	$\|\Gamma_{MAX}\|$ 3-stub 11 switches	$\|\Gamma_{MAX}\|$ 3-stub 13 switches	$\|\Gamma_{MAX}\|$ 2-stub 11 switches	$\|\Gamma_{MAX}\|$ 1-stub 10 switches
6	0.77	0.77	0.95	0.86
8	0.92	0.92	0.94	0.69
12	0.92	0.92	0.91	0.93
16	0.95	0.95	0.93	0.91
20	0.96	0.97	0.96	0.97
30	0.95	0.97	0.99	0.98

VII. INTERMODULATION MEASUREMENTS

The intermodulation analysis of MEMS switches, and varactors is presented in [15] and show that MEMS-based circuits generate insignificant amount of intermodulation products, especially if the frequency difference between the two RF signals (Δf) is higher than the mechanical resonant frequency of the bridge. The intermodulation measurements of the impedance tuners were carried out with the measurement set-up shown in Fig. 19, and the circuits were terminated with either a 50 Ω load or with a short circuit. In the case of the short circuit condition, the generated intermodulation signals (IM3 products) were measured at the input port using a circulator.

The triple-stub tuner with 11 switched-capacitors was measured at 8 and 17 GHz, and the measurement IIP3 is > 35 dBm for a 5 kHz separation frequency, even under short circuit conditions (Fig. 20). Fig. 20 also shows that the intermodulation products are higher at 17 GHz than at 8 GHz as predicted in [15]. Also, the IIP3 increases as $(\Delta f)^4$ and therefore it can be expected to be > +60 dBm for a Δf of 1 MHz. This is so low that it is simply un-measurable in most experimental set-ups. These findings confirm the results of [15].

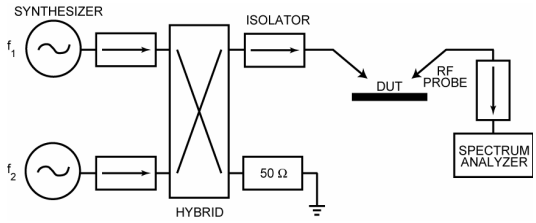

Figure 19. Schematic of the intermodulation measurement set-up.

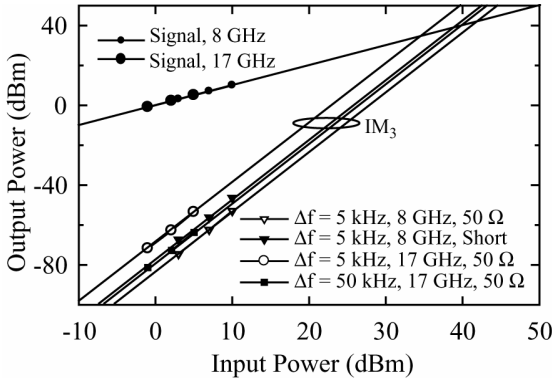

Figure 20. Measured third-order intermodulation of the triple-stub tuner with 11 switched capacitors at 8 and 17 GHz, when all the switches were in the up-state.

VIII. POWER HANDLING

Power handling is not a critical issue if the tuners are used in noise parameter measurements. However, in load-pull measurements, power handling can be important especially if the tuners are used at the output port. As is well known [14], if a DC or an RF voltage is applied between the electrodes of a MEMS switch, the position of the switch changes since the electrostatic force is dependent on V^2, and this translates to V_{rms}^2 for RF voltages. The MEMS switch is pulled down if $|V_{\text{rms}}|$ is equal or greater than the DC pull-down voltage of the switch. Another problem related to high RF power is the hold-down voltage in the down-state position [15].

The power handling measurement set-up is shown schematically in Fig. 21, where isolators were used for achieving a 50 Ω system at the source and the power meter. The power handling of the triple-stub tuner with 11 switched capacitors was measured at 8 and 17.6 GHz (Fig. 22). The triple-stub tuner circuits can handle up to 23-24 dBm RF power at 8-17 GHz depending on the switch combination. This is enough for most transistors operating at this frequency band at the input port or as a tuner in noise parameter measurements, but this is not enough for an output port matching network.

The voltages and currents across the switched capacitors were simulated using Agilent ADS with 24 dBm RF power (Fig. 23). The simulation predicts that switches S1 and S2 have the highest rms voltage (5 V). In this case, the pull-down voltage of the switches was closer to 10 V and a 5-6 V RF rms voltage will start to change the switch capacitance. However, this is not a complete solution, since it is assumed that the circuit is not changing, but as the bridge position and capacitance changes, the voltage distribution on the circuit changes, and may result in a higher voltage across S1 and S2. This means that a coupled microwave-circuit/mechanical-analysis solution is needed to find the behavior of the reconfigurable circuit in a dynamic fashion, and this is not done here.

For higher power handling, it is recommended that the MEMS switches are fabricated with a high pull-down voltage (30 V instead of 10-15 V). This will increase the power handling by a factor of 4 to around 30 dBm. A potential problem which may arise from using 30-40 V bias voltages is the charging of the dielectric layer in the MEMS switch, but this is mitigated by the use of a thick SiN dielectric layer (3500 Å instead of the standard 1000 Å) since the design does not necessitate a large capacitance ratio. The currents in the switches are quite low, in the both the up-state and down-state positions, and remain lower than 150 mA rms for virtually all switch combinations up to 30 dBm.

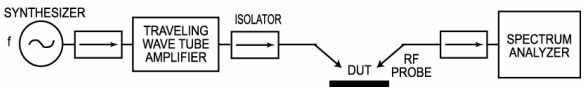

Figure 21. Schematic drawing of the power handling measurement set-up.

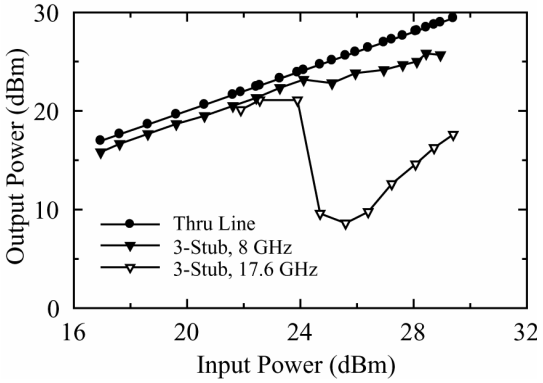

Figure 22. Measured power handling of the triple-stub tuner with 11 switched capacitors at 8 and 17.6 GHz, when all of the switches were in the up-state position. In this case, a 24 dBm power handling is observed.

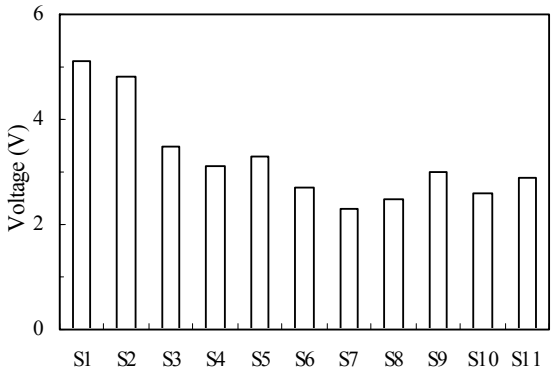

Figure 23. Simulated rms voltage across the switched capacitors in the triple-stub tuner with 11 switched capacitors at 17.6 GHz with 24 dBm input RF power. All swtches were in the up-state in the simulations.

IX. CONCLUSIONS

This paper presented a whole set of impedance tuners for 6-24 GHz applications using single-, double-, and triple-stub topologies. The essential idea of the design is that switched capacitors with a relatively low capacitance ratio are used (and not switches), which results in a very large number of impedance combinations (1024-8192 different impedances for 10-13 switched capacitors). The switched capacitors were used for changing the electrical lengths and impedance of stubs and sections between the stubs. The measured impedance and frequency coverage of these tuners is the widest to-date from any integrated tuner at this frequency range. Also, these tuners can achieve a very high VSWR over a wide frequency range, and the double-stub tuner resulted in a measured VSWR of 199 at 30 GHz. The areas of the single and double-stub tuners are small enough to be integrated inside on-wafer measurement probes to increase the measurement accuracy and automation in noise parameter or load-pull measurements systems. If the stub-based tuners are used as matching networks with amplifiers, the single-stub topology should be used to get the lowest loss. The tuners can be scaled up to 120 GHz and this work has been presented in [17-19].

ACKNOWLEDGEMENTS

This work has been supported by the ESA/ESTEC contract no. 1655/95/NL/MV at MilliLab, VTT, and the DARPA IRFFE program at the University of Michigan.

REFERENCES

1. M. Kantanen, M. Lahdes, T. Vähä-Heikkilä, and J. Tuovinen, A wideband automated measurement system for on-wafer noise parameter measurements at 50-75 GHz, IEEE Transactions on Microwave Theory and Techniques, vol. 51, no. 5, 2003, pp. 1489-1495.
2. T. Vähä-Heikkilä, M. Lahdes, M. Kantanen, and J. Tuovinen, On-wafer noise parameter measurements at W-band, IEEE Transactions on Microwave Theory and Techniques, vol. 51, no. 6, 2003, pp. 1621-1628.
3. M. Pierpoint, R.D. Pollard, and J.R. Richardson, An automated measurement technique for measuring amplifier load-pull and verifying large-signal device models**,** IEEE MTT-S International Microwave Symposium Digest, vol. 86, Baltimore, Maryland, 1986, pp. 625 - 628.

4. W. Bischof, Variable impedance tuner for MMIC's, IEEE Microwave and Guided Wave Lett., vol. 4, no. 6, pp. 172-174, 1994.
5. C.E. McIntosh, R.D. Pollard, and R.E. Miles, Novel MMIC source-impedance tuners for on-wafer microwave noise-parameter measurements, IEEE Transactions on Microwave Theory and Techniques, vol. 47, no. 2, 1999, pp. 125-131.
6. H.-T. Kim, S. Jung, K. Kang, J.-H. Park, Y.-K. Kim, and Y. Kwon, Low-loss analog and digital micromachined impedance tuners at the Ka-band, IEEE Transactions on Microwave Theory and Techniques, vol. 49, no. 11, 2001, pp. 2394-2400.
7. J. Papapolymerou, K. L. Lange, C. L. Goldsmith, A. Malczewski, and J. Kleber, Reconfigurable double-stub tuners using MEMS switches for intelligent RF front-ends, IEEE Transactions on Microwave Theory and Techniques, vol. 51, 2003, pp. 271-278.
8. R. E. Collin, Foundations for Microwave Engineering, 2nd edition, New York, McGraw-Hill, 1992.
9. T. Vähä-Heikkilä, J. Varis, J. Tuovinen, and G.M. Rebeiz, A reconfigurable 6-20 GHz RF MEMS impedance tuner, IEEE MTT-S International Microwave Symposium digest, Forth Worth, TX, USA, 2004, pp. 729–732.
10. T. Vähä-Heikkilä, and G.M. Rebeiz, A 20-50 GHz reconfigurable matching network for power amplifier applications, IEEE MTT-S International Microwave Symposium digest, Forth Worth, TX, USA, 2004, pp. 717-721.
11. T. Vähä-Heikkilä and G.M. Rebeiz, A 4-18 GHz reconfigurable RF MEMS matching network for power amplifier applications, International Journal of RF and Microwave Computer-Aided Engineering," vol. 14, no. 6, 2004, pp. 356-372.
12. Q. Shen and N.S. Barker, A reconfigurable RF MEMS based double slug impedance tuner, Proceedings of the 35th European Microwave Conference, Paris, France, 2005, pp. 537-540.
13. J. B. Rizk, W-band RF MEMS Switches, Phase Shifters and Antennas, Ph.D. dissertation, Dept. Elect. Eng. Univ. of Michigan at Ann Arbor, MI, 2003.
14. S. Van den Bosch and L. Martens, Improved impedance-Pattern Generation for Automatic Noise-Parameter Determination, IEEE Transactions on Microwave Theory and Techniques, vol. 46, no. 11, 1998, pp. 1673-1678.
15. L. Dussopt and G.M. Rebeiz, Intermodulation distortion and power handling in RF MEMS switches, varactors and tunable filters, IEEE Transactions on Microwave Theory and Techniques, vol. 51, no. 4, 2003, pp. 1247-1256.
16. G.M. Rebeiz, RF MEMS: Theory, Design, and Technology, John Wiley & Sons, New York, 2003.
17. T. Vähä-Heikkilä, J. Varis, J. Tuovinen, and G.M. Rebeiz, A 20-50 GHz RF MEMS single-stub impedance tuner, IEEE Microwave and Wireless Components Letters, vol. 15, no. 4, 2005, pp. 205-207.
18. T. Vähä-Heikkilä, J. Varis, J. Tuovinen, and G.M. Rebeiz, A V-band single-stub RF MEMS impedance tuner, Proceedings of the 34th European Microwave Conference, Amsterdam, Netherlands, 2004, pp. 1301–1304.
19. T. Vähä-Heikkilä, J. Varis, J. Tuovinen, and G.M. Rebeiz, W-band RF MEMS double- and triple-stub impedance tuners, IEEE MTT-S International Microwave Symposium 2005, Long Beach, CA, June 2005, pp. 923-926.